Int. J. Electrochem. Sci., 14 **(2019)** 2452 – 2461, doi: 10.20964/2019.03.50

International Journal of
ELECTROCHEMICAL
SCIENCE
www.electrochemsci.org

Preparation and Electrochemical Properties of Bamboo-based Carbon for Lithium-Ion-Battery Anode Material

Ruiqi Su, Xianming Dong[*]

College of Materials and Energy, South China Agricultural University, Guangzhou 510642, China
[*]E-mail: dongxming@263.net

Received: 6 September 2018/ *Accepted:* 24 January 2019 / *Published:* 7 February 2019

In this study, we use bamboo as a raw material and KOH as an activator to prepare a bamboo-based carbon anode material for use in lithium-ion batteries by applying the microwave radiation method. The crystal structure and morphology of the prepared material are characterized by X-ray diffraction and scanning electron microscopy, respectively, and the electrochemical performance of the material is characterized by galvanostatic charge–discharge and cyclic voltammetry. The results demonstrate that the bamboo-based carbon material can be used as an anode material with high electronic and ionic conductivity in LIBs. The initial charge and discharge capacities of the bamboo-based activated carbon material at 0.5 C range up to 961.4 and 2071 $mA \cdot h \cdot g^{-1}$, respectively. The first charge and discharge Coulombic efficiency is only 46.4%, and after 100 cycles, the circulation charge and discharge capacities remain at 721.8 and 737.3 $mA \cdot h \cdot g^{-1}$, respectively. Overall, the efficiency remains above 97.8%, which demonstrates the excellent cycling stability of the bamboo-based carbon material. The sample shows good rate performance and excellent cycle stability because of the large specific surface area, which can improve the permeability of electrolyte, increase the reactive sites, and improve the electrochemical performance.

Keywords: Bamboo; Lithium-ion battery; Carbon materials; Microwave radiation; Electrochemical properties

1. INTRODUCTION

With the alarming increase in the severity of the global energy crisis, scientists worldwide have increasingly turned to the research and development of new forms of renewable clean energy. In this regard, lithium-ion batteries (LIBs) have become the primary choice for “green” batteries owing to their high energy density, non-polluting nature, and high secondary-utilization rate [1]. The LIB anode material is one of the key factors for its performance, among which carbon-based materials are the most commonly used materials in these research and applications [2,3]. Graphite has been

commercialized as a LIB anode material owing to its high efficiency and good cycling performance. However, the theoretical specific capacity of graphite is only 372 $mA \cdot h \cdot g^{-1}$ [4]. Graphite has also been shown to exhibit relatively poor charge and discharge performance between the electrodes and electrolyte at high C-rates [5], which prevent it from satisfying the demand of high energy storage for electric vehicles of the future. Therefore, exploring new anode materials for such applications is necessary [6-9]. In addition to graphite, several activated carbon materials such as coal-based and rice-husk activated carbon materials have been investigated as anode materials [10]. Meanwhile, as a cathode material of a LIB, biomass carbon exhibits the characteristics of higher energy density, greater stability, and safer operation. Such use of carbon from waste recycling can not only reduce environmental pollution but also achieve green energy, which finds broad usages in LIBs, fuel cells, supercapacitors, and other applications [11]. Porous biomass carbon prepared from corn straw exhibits the characteristics of adjustable pore-size distribution, high specific surface area, large pore volume, and good electrical and thermal conductivities, which can not only effectively inhibit the growth of lithium dendrites but also provide more lithium-ion transfer channels [12-14]. In this regard, Wang et al. [15] synthesized a porous carbon material from rice husk. When used as a cathode material for LIBs, the LIB discharge capacity at a current density of 10 C was observed to be 137 $mA \cdot h \cdot g^{-1}$. Li et al. prepared amorphous carbon from rice husks, whose reversible capacity was 502 $mA \cdot h \cdot g^{-1}$ after 100 cycles at a current density of 0.2 C [16]. However, the reversible capacity of such cathode materials was not high, and the resulting cyclic performance was unstable.

China is one of the major sources of bamboo, where large volumes of bamboo scraps (usually as garbage and burned bamboo) currently form bulk waste that results in soil acidification and environmental pollution. By preparing carbon materials from bamboo, scientists can fully use natural resources, minimize waste, and meet sustainable development requirements. Against this backdrop, in this paper, we report the preparation and electrochemical properties of a bamboo-based carbon material for application to LIBs, whichin we use bamboo charcoal as a raw material, KOH as an activating agent, and microwave irradiation for synthesis.

2. EXPERIMENTAL

2.1. Preparation of samples

The bamboo pieces used in this study were first passed through a 200-mesh sieve. The sieved pieces were placed in a crucible installed in a laboratory-assembled microwave device rated at 900 W. The sorted bamboo pieces were heated for 10 min for carbonization to occur and to form a carbon precursor. After cooling, the carbon precursor was ground using an agate mortar and subsequently sequentially soaked in concentrated HNO_3 and HF for 12 h. The acid-soaked pieces were filtered and washed to regain their neutral pH, followed by drying at 90 °C. Next, 1 g of the processed carbon precursor and 4 g of KOH (used as an activator) were evenly mixed in the agate mortar, and the mixture was transferred to a 30 mL crucible that was placed in the microwave. After activation for 10 min at 900 W, the sample was cooled to room temperature. The sample was soaked, filtered, and subsequently washed with distilled water and 1 $mol \cdot L^{-1}$ HCl until a neutral pH was obtained. After drying, a sample of the bamboo-charcoal-based material was obtained.

2.2. Characterization

The structure of the sample was analyzed using X-ray diffraction (XRD; D2, Bruker, Germany) with Cu K_α radiation in the 2θ range of 10°–70° with a step size of 0.02° at 30 kV and 10 mA. The material was characterized by Raman spectroscopy (Senterra, Bruker, Germany) using a 512 nm laser in the scanning range of 1000–2000 cm^{-1}. The morphology of the sample was observed using scanning electron microscopy (SEM, Hitachi S-4800, Japan). For the electrochemical measurements, an anode slurry was prepared by mixing the active material (80 wt%), acetylene black (15 wt%), and polytetrafluoroethylene (5 wt%) in deionized water. The obtained slurry was pasted on an aluminum foil, which was subsequently cut into disks with a diameter of 10 mm, and dried in a vacuum oven at 110 °C for 12 h. Finally, 2025-type cells were assembled in an argon-filled glove box, which used a lithium foil as a positive electrode, $LiPF_6$ (1 $mol \cdot L^{-1}$) mixed with a solution of ethylene carbonate (EC), dimethyl carbonate (DMC), and ethyl methyl carbonate (EMC) (EC/DMC/EMC volume ratio of 1:1:1) as an electrolyte, and Celgard 2400 as a separator. The charge–discharge profiles of the cells were acquired using a battery-testing system (LAND CT-2001A, Wuhan LAND Electronics Co., Ltd., China), which operated in the voltage range of 0.02–3.5 V at 25 °C. The cyclic voltammetry (CV) (LK2005) curves were obtained at a scan rate of 0.1 $mV \cdot s^{-1}$.

3. RESULTS AND DISCUSSION

Figure 1 shows the XRD patterns of the sample subjected to various treatment processes. Curve "a" in Figure 1 shows the XRD pattern of the raw material (bamboo) after carbonization by microwave irradiation. The impurity peaked at 26.7°, 28.1°, and 28.7°, which corresponded to the diffraction due to inorganic salts of sulfur, phosphorus, and nitrogen, in the bamboo. Figure 1(A) shows the XRD patterns of the bamboo after it was soaked in HF only, in HNO_3 only, and sequentially in HF and HNO_3. We note that the diffraction peaks of the inorganic salts remained after treatment in HF or HNO_3 only. After successive leaching in the HF and HNO_3 solutions, the diffraction peaks of the impurities disappeared, and the XRD pattern exhibited a smooth curve. These results explained the necessity to remove impurities from the raw material (bamboo) using preliminary treatments. On the basis of these results, we applied the combined treatment of HNO_3 and HF in this study to prepare the sample for subsequent experiments. Figure 1(B) shows the XRD pattern obtained after successively leaching the raw material in HNO_3 and HF for 12 h, as indicated by Curve "b." Figure 1(B) shows the XRD curve of the bamboo-based activated carbon after the KOH–bamboo-precursor mixture (mixing ratio of 4:1) was activated for 10 min in the microwave at 900-W power, designated as Curve "c." From the figure, we note that no obvious changes were observed in the XRD patterns obtained before and after activation of the bamboo-based carbon material, thereby indicating that KOH activation of the bamboo-based carbon precursor did not drastically change the amorphous structure of the raw material. When compared with the XRD pattern of an inactive bamboo-based material, the intensities of the diffraction peaks of the XRD pattern after activation appeared to decrease, possibly due to the diffusion of K vapor into the bamboo carbon layer during activation by KOH. Another reason may be the effect of corrosion by KOH, which led to an increase in the surface area of the bamboo charcoal

material. This effect indicates that the microcrystalline structure of the activated bamboo-based carbon material was closer to that of amorphous carbon than of graphite [17].

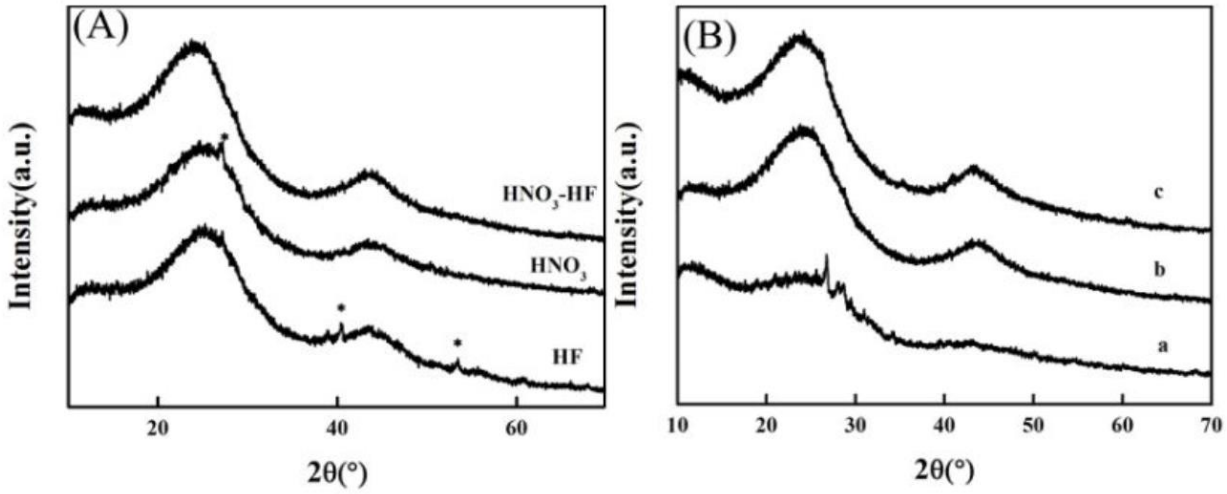

Figure 1. (A) XRD patterns of the bamboo-based carbon material after treatment in HF only, in HNO_3 only, and in both HNO_3 and HF. (B) XRD patterns of the bamboo-based carbon material (a) after carbonization and before acid treatment for impurity removal, (b) after successive leaching in HNO_3 and HF for 12 h, and (c) after activation.

Next, we conducted a Raman analysis to determine the degree of graphitization of the bamboo charcoal. Figure 2 shows that two Raman peaks appeared at wavenumbers of 1361 and 1591 cm^{-1} in the Raman spectrum of the bamboo-based carbon material. For the graphite materials, only one sharp Raman peak appeared at 1591 cm^{-1} (commonly referred to as the G band). For the amorphous carbon materials, the peak at 1361 cm^{-1} originated from the structural defects, and this peak (referred to as the D band) is commonly used to represent the disorder of a material. Therefore, the ratio (R) between the intensities of the peaks at 1361 and 1591 cm^{-1} can be used to characterize the degree of graphitization of a carbon material. A higher degree of graphitization corresponds to a larger crystallite size and smaller value of R. Therefore, when R (= I1361/I1591) is less than one, the degree of graphitization is not high [18]. In our present study, the observed low degree of graphitization may be due to the introduction of a large number of functional groups in the bamboo charcoal during any or all of the carbonization, acid treatment, and activation processes [19].

Figure 3 shows the SEM images of the sample acquired to study the sample morphology. The bamboo charcoal appeared as a thin transparent porous material, which may be due to the corrosive effects of the KOH activation resulting from the increase in the microwave-radiation duration. When the activation temperature was increased, the number of carbon atoms in the activated state increased. Figure 3 also shows that the prepared bamboo matrix carbon material exhibited a highly porous structure, and the lamellar and pore structures intersected to form a large number of “slits”, which resulted in a higher specific surface area of the sample.

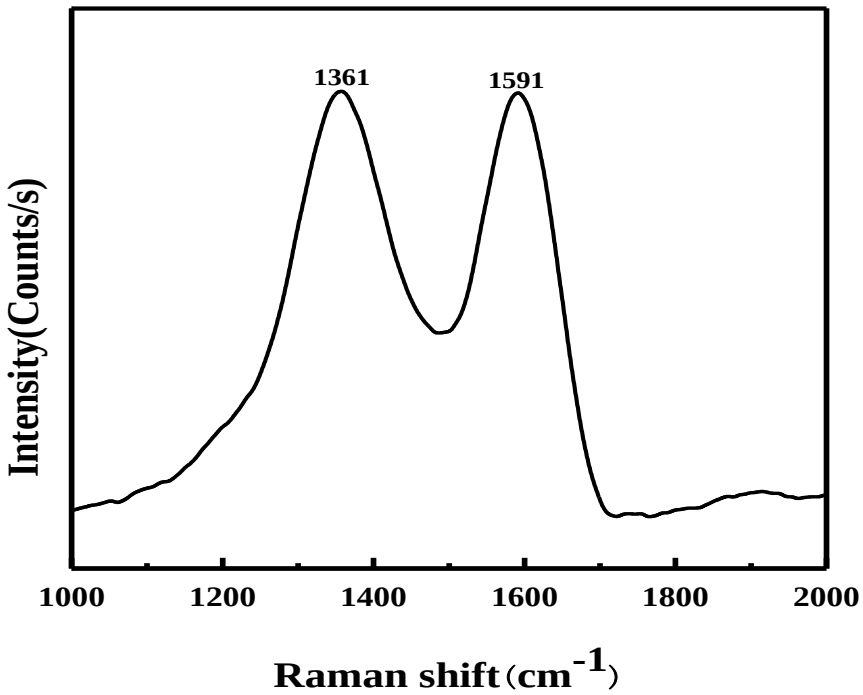

Figure 2. Raman spectra of the bamboo-based carbon material using a 512 nm laser at the scanning range of 1000-2000 cm^{-1}.

Thus, the contact area and permeability between the reactant and electrolyte increased. Further, these slits provided a larger amount of free movement space for lithium ions to be embedded and released, which is beneficial for improving the specific capacity and cycling stability of the samples.

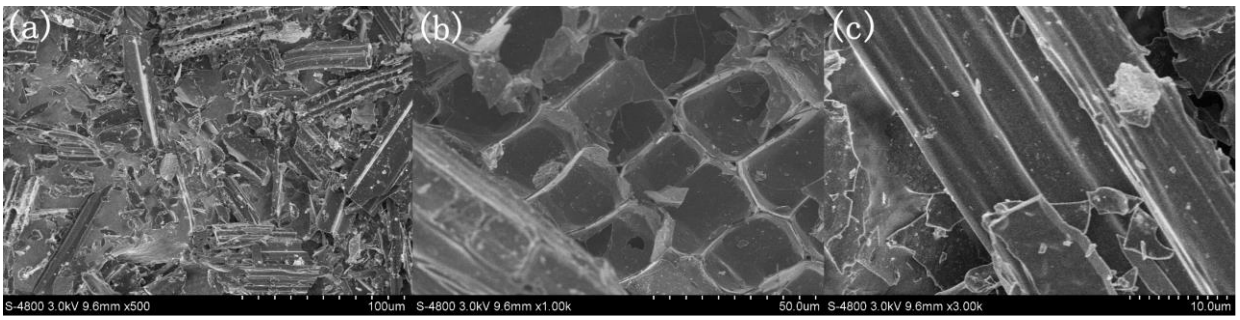

Figure 3. Scanning-electron micrographs of the bamboo-based carbon materials.

By using bamboo carbon as an electrode material of a LIB, we next tested the battery electrochemical performance in the voltage range of 0.02–3.5 V at a current density of 1 C. The corresponding results are shown in Figure 4. The current density was 1 C at the 2nd, 50th, and 100th cycle of the test. The charge–discharge curves indicate that the first-cycle discharge capacity was as large as 2071 $mA{\cdot}h{\cdot}g^{-1}$, the first-charge capacity was 961.4 $mA{\cdot}h{\cdot}g^{-1}$, and the Coulombic efficiency was only 46.4%, which indicated a high irreversible capacity. In the second cycle, the discharge capacity reached 979.5 $mA{\cdot}h{\cdot}g^{-1}$, which was significantly higher than the theoretical discharge capacity of graphite (372 $mA{\cdot}h{\cdot}g^{-1}$). From the start of the second cycle, the discharge capacity remained stable, which greatly improved the Coulombic efficiency. After 100 cycles, the charge capacity was 721.8 $mA{\cdot}h{\cdot}g^{-1}$, the discharge capacity was 737.3 $mA{\cdot}h{\cdot}g^{-1}$, and the efficiency was

maintained at 97.8%, thus indicating a good cycle stability. We speculate that this result could be because all the deintercalated lithium ions could not be reversibly embedded during the first cycle. As the cycles progressed, the electrode materials and electrolyte came in full contact with each other, the capacitance gradually stabilized, and the charge–discharge efficiency gradually increased. Simultaneously, we note that Figure 4 shows skewed smooth curves and does not show any obvious plateaus corresponding to material discharge mainly because of the multiple electrochemical processes at different potentials, surface functional groups, and presence of defects [20,21].

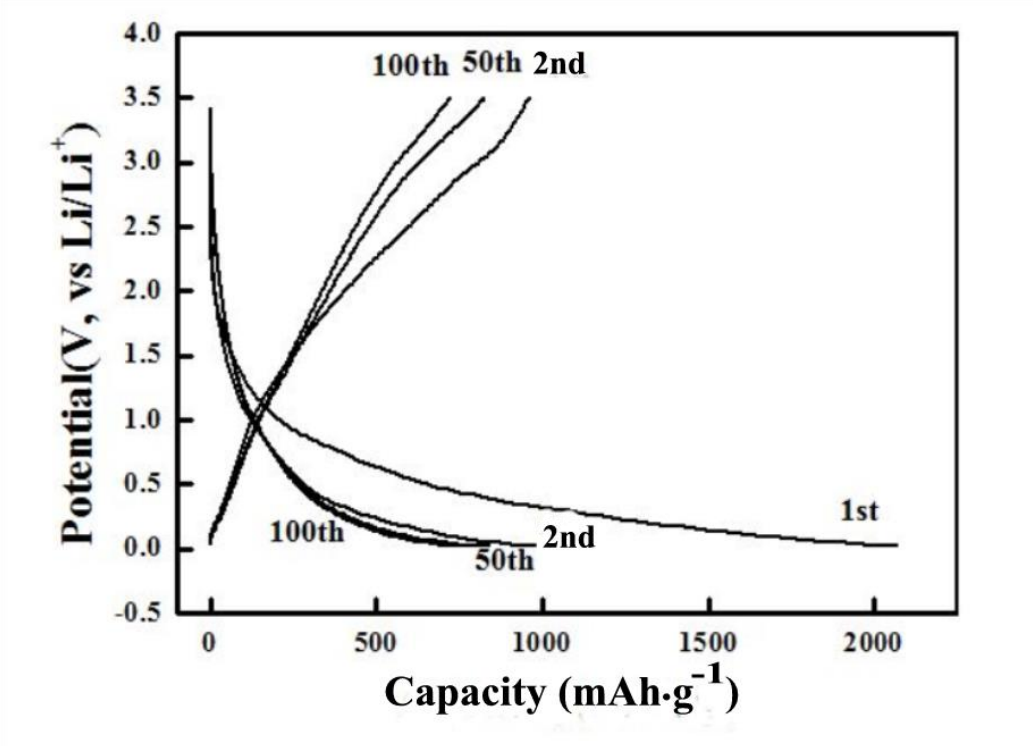

Figure 4. Charge–discharge curves of the bamboo-based carbon material at the current density of 0.5 C and the potential range of 0.02–3.5 V

Figure 5 shows the charge–discharge curves of the bamboo-based carbon material in the voltage range from 0.02 to 3.5 V. When the charge and discharge rates were 0.5 C, 1 C, 2 C, 5 C, and 10 C, the discharge capacities were 979.5, 650.8, 559.7, 447.5, and 296.6 $mA \cdot h \cdot g^{-1}$, respectively. The high efficiency of the charge and discharge properties could be explained by the lamellar porous structure of the material. This porous electrode material facilitated reduction in the resistance against the active material and contributed to the rapid insertion and detachment of lithium ions. The presence of the porous structure effectively reduced the reaction and transfer resistances of the charges and increased the specific surface area of the bamboo-based carbon material, thus improving the electrochemical properties [21]. The excellent electrochemical properties of the material further confirmed the positive influence of the pore structure observed in the SEM images.

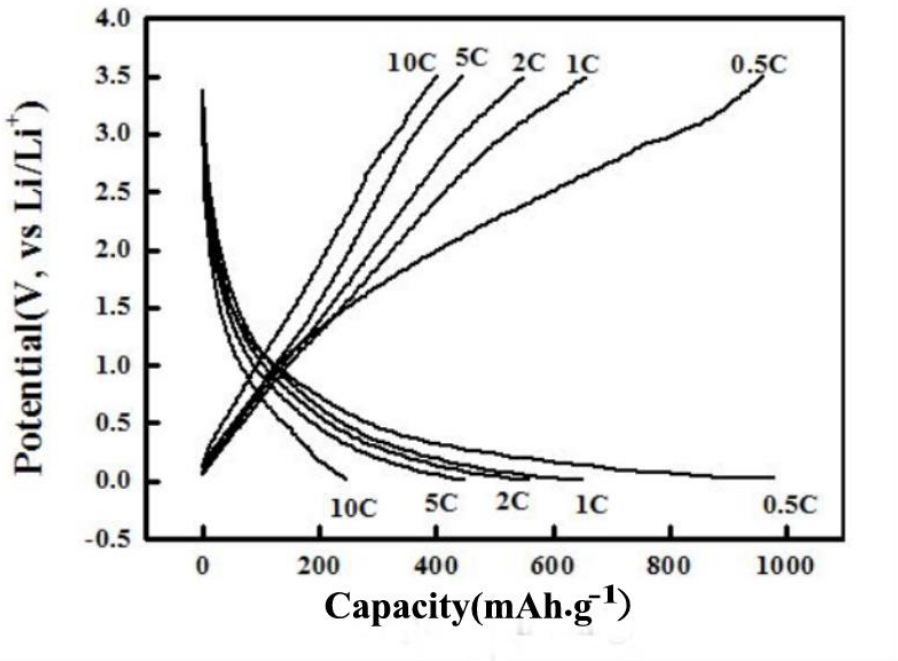

Figure 5. Charge–discharge curves obtained at various discharge-current densities of the bamboo-based carbon material at the potential range of 0.02–3.5 V.

Figure 6 shows the life cycle diagram of the LIB constructed using a bamboo-based carbon material as its electrode. The charge–discharge rates of the battery were varied at 0.5 C, 1 C, 2 C, 5 C, and 10 C. Figure 4 shows that when the charge–discharge rate was 0.5 C, the discharge capacity of the first-cycle discharge of the bamboo-based carbon material was 2071 $mA{\cdot}h{\cdot}g^{-1}$. After 100 cycles, the capacity was 737.3 $mA{\cdot}h{\cdot}g^{-1}$, which was significantly higher than the theoretical specific discharge capacity of a graphite cathode (372 $mA{\cdot}h{\cdot}g^{-1}$). Even at a high current density of 10 C, the discharge capacity of the material remained at approximately 244.5 $mA{\cdot}h{\cdot}g^{-1}$. The discharge capacity of the material was 716.2 $mA{\cdot}h{\cdot}g^{-1}$ when the charge–discharge rate was again reduced to 0.5 C after cycling through the rates of 1 C, 2 C, 5 C, and 10 C. These results indicate that when a bamboo-based carbon material is used as the anode material of a LIB, the battery exhibits good cycling stability and excellent rate performance.

Figure 7 shows the cyclic voltammogram of the prepared material. The scanning voltage range was 0.02–3.0 V, and the scan rate was 0.1 $mV{\cdot}s^{-1}$. The figure shows that the first curve exhibited two obvious reduction peaks between 0.50–0.85 V and 1.00–1.50 V. Among them, the reduction peak between 1.00 and 1.50 V was weak, which represented the formation of a solid electrolyte interface (SEI) film on the electrode surface and irreversible decomposition of the electrolyte solution. The reduction peak between 0.50 and 0.85 V was strong and could be attributed to the complex irreversible reaction of lithium ions on the surface of the carbon material [22]. However, no corresponding oxidation peak was present in the oxidation stage of the curve, and the two reduction peaks did not appear in the subsequent cycle. Therefore, the irreversible capacity of the bamboo carbon material in the first cycle could be attributed to the two irreversible reactions in this process [23]. From close observation of the curve, we can see that a sharp reduction peak appeared near 0 V, which corresponded to the process of lithium-ion embedment in the electrode, and a gentle oxidation peak

was observed between 0. 15 and 0.50 V, which corresponded to the lithium-ion detachment from the electrode [22]. In the pyrolysis and carbonization processes, a large number of pore structures were formed in the interior of the carbon materials. The embedding and release of lithium ions in the pores corresponded to the emergence of bumps in the curve, and thus, an obvious bump was present in the range of 1.0–1.3 V. Simultaneously, the curves of the first three cycles tended to coincide, which indicated that a stable SEI film was formed on the electrode surface and that the electrode material structure was relatively stable [24].

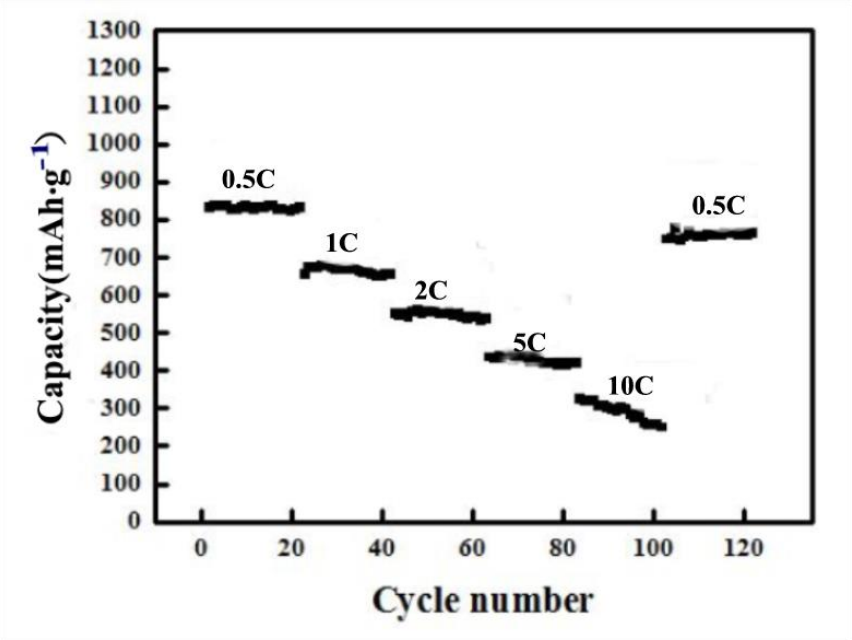

Figure 6. Cycle performance of a bamboo-based carbon material at the potential range of 0.02–3.5 V

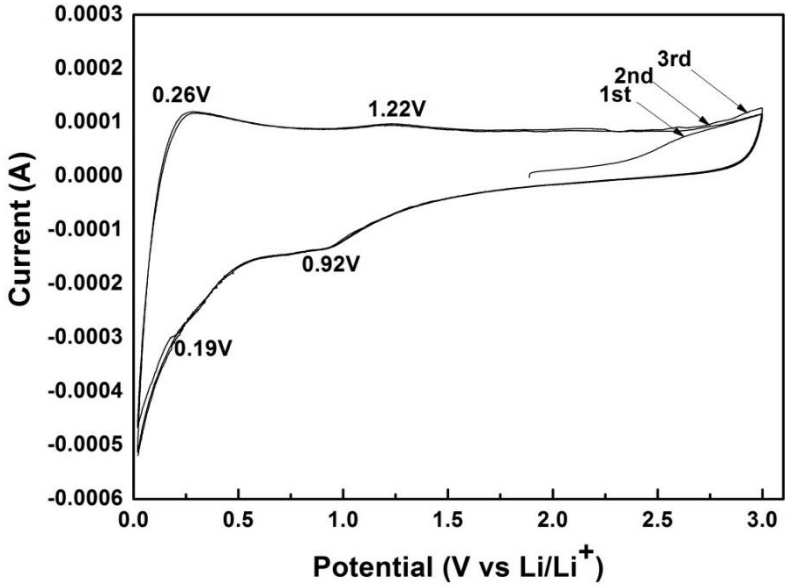

Figure 7. Cyclic voltammetry curves of the bamboo-based carbon materials at a scan rate of 0.1 mV·s^{-1} in the potential range of 0.02 to 3.0 V

4. CONCLUSION

In this study, we used bamboo as a carbon source, KOH as an activator, an alkali-to-carbon ratio of 4:1, and microwave irradiation at 900 W for dehydrogenation to prepare a bamboo-based carbon anode material for LIB applications. We also prepared a graphite crystallite structure of amorphous carbon material after 10 min of carbonization and activation. Sample characterization using XRD, Raman spectroscopy, and SEM indicated that the bamboo carbon material was successfully synthesized. Our electrochemical tests indicated that the bamboo charcoal material exhibited excellent electrochemical performance. At a rate of 0.5 C of the bamboo-carbon-based LIB, the discharge specific capacity was 2071 $mA{\cdot}h{\cdot}g^{-1}$, and the charge capacity was 961.4 $mA{\cdot}h{\cdot}g^{-1}$. The Coulombic efficiency in the charge and discharge processes for the first cycle was only 46.4%, which indicated the presence of a large irreversible capacity. However, the charging capacity remained at 721.8 $mA{\cdot}h{\cdot}g^{-1}$ after 100 cycles, the discharge specific capacity remained at 737.3 $mA{\cdot}h{\cdot}g^{-1}$, and the efficiency subsequently remained at more than 97.8%, which indicated good cycle stability. The cycle stability and rate performance could be attributed to the formation of a larger number of slits because of the intersection of the porous and lamellar carbon structures, thereby leading to a high specific surface area, increase in the reactant and electrolyte contact area, and permeability for lithium-ion embedment and release because of the greater freedom of ion movement. In summary, we believe that the use of bamboo-based carbon anodes can further contribute to the development of green batteries.

ACKNOWLEDGEMENT
This study was supported by the science and technology project of Guangdong (2015B020237009, 2016A010103024) and the Education Ministry of China and the College Students' Innovative Entrepreneurial Training Project of Guangdong (201710564297).

References

1. Y.J. Wei, H. Ehrenberg, N.N. Bramnik, K. Nikolowski, C. Baehtz, H. Fuess, *Solid State Ionics*, 178 (2007) 253.
2. J.S. Kim, W.Y. Yoon, K.S. Yoo, G.S. Park, C.W. Lee, Y. Murakami, D. Shindo, *J. Power Sources*, 104 (2002) 175.
3. D.S. Su, R. Schlögl, *ChemSusChem.*, 3 (2010) 136.
4. J.M. Tarascon, M. Armand, *Nature*, 414 (2001) 359.
5. Z.H. Yu, F. Wu, *New Carbon Mater.*, 17 (2002) 29.
6. H.S. Kim, S.G. Kwon, S.H. Kang, Y. Piao, Y.E. Sung, *Electrochim. Acta*, 136 (2014) 47.
7. A.L.M. Reddy, A. Srivastava, S.R. Gowda, Y.Z. Piao, Y.E. Sung, *ACS Nano*, 4 (2010) 6337.
8. C.K. Chan, H. Peng, G. Liu, K. McIlwrath, X.F. Zhang, R.A. Huggins,Y. Cui, *Nat. Nanotechnol.*, 3 (2008) 31.
9. P.L. Taberna, S. Mitra, P. Poizot, P. Simon, J.M. Tarascon, *Nat. Mater.*, 5 (2006) 567.
10. Y.F. Ma, L.J. Chen , B.L. Xing , B. Xu , G.H. Huang, C.X. Zhang, *J. China Coal Soc.*, 37(2012) 472.
11. B. Hu，S. H. Yu, K. Wang，L. Liu，X. W. Xu, *Dalton Trans*., 40(2008)5414
12. Q .Huang，S. Wang，Y. Zhang，B. Yu，L. Hou，G. Su，*J．Phys．Chem*., 6(2016)3139
13. N. P. Wickramaratne，J. Xu，M. Wang，L. Zhu，L. Dai，*Chem．Mater*., 9(2014)2820

14. B. Wen，S. Wei，Z. Shi，H. B. Lin，H. Y. Lu，*Chem． J． Chinese U*，3(2013)674
15. L. Wang，Z. Schnepp，M. Titirici，*J． Mater． Chem*., 17(2013)5269
16. Y. Li，F. Wang，J. Lian，X. Hu，K. Yu，*New J． Chem.,* 1(2016)325
17. H. Dong, Y. Zhang, L. Wang, A. Zhang, Y. Song, X. Li, *Inorg. Chem. Ind.*, (2010)
18. F. Tuinstra, J.L. Koenig, *J. Compos. Mater*., 4 (1970) 492.
19. L.X. Zhu, Y.Z. Li, X. Zhao, Q.H. Zhang, *Chem． J． Chinese U* , 33 (2012) 1804.
20. P. Lian, X. Zhu, S. Liang, S. Li, W. Yang, H. Wang, *Electrochim. Acta*, 55 (2010) 3909.
21. M. Liang, L. Zhi, *J. Mater. Chem.*, 19 (2009) 5871.
22. W. L. Song，L. Z. Fan, M. S. Cao，*J． Mater． Chem.,* 25(2014)5057
23. F. D. Han，Y. J. Bai，R. Liu，B. Yao，Y. X. Qi，N. Lun，*Adv． Energy Mater*., 5(2011)798
24. Y. Li ，C. Li，K. F. Yu，*Chem． J． Chinese U*，4(2018)607